

NUMERICAL INVESTIGATION ON THERMAL PERFORMANCE AND FLOW CHARACTERISTICS OF Z AND S SHAPE PRINTED CIRCUIT HEAT EXCHANGER USING S-CO₂

by

Yuan-Sheng LIN^{a,b}, Qi JING^a, and Yong-Hui XIE^{a*}

^a School of Energy and Power Engineering, Xi'an Jiaotong University, Xi'an, China

^b Key Laboratory of Thermal Power Technology,
Wuhan Second Ship Design and Research Institute, Wuhan, China

Original scientific paper
<https://doi.org/10.2298/TSCI180620090L>

As a high-efficiency compact heat exchanger, the printed circuit heat exchanger has been widely applied into nuclear reactor and energy industry. In the present paper, the thermal hydraulic performance of printed circuit heat exchanger based on S-CO₂ Brayton power cycle has been numerically investigated for various channel shape and bend angle. A total of seven different shaped channels including straight, Z-10, Z-20, Z-30, S-10, S-20, S-30 are modeled, and evaluated according to the heat transfer and friction performances within the Reynolds number of 5000-30000. The inlet temperature/outlet pressure of hot channel and cold channel are 553 K/2.6 MPa and 381 K/8.5 MPa, respectively. The flow patterns, average Nusselt number, friction factor, and heat exchanger effectiveness are obtained. On the comprehensive consideration of heat transfer enhancement and friction, the S-20 channel produces the best thermal performance. This investigation has provided important reference data for the design of advanced printed circuit heat exchanger in the energy industry.

Key words: *printed circuit heat exchanger, supercritical CO₂, thermal hydraulic performance, S shape channel, Z shape channel*

Introduction

With the rapid development of turbomachinery and nuclear energy industry, the heat load of the system key equipment increases gradually. As a heat transfer component widely applied in the energy field, the heat exchanger is faced with huge challenges. For most engineering equipment, the physical spaces are limited. Thus, for the design of heat exchanger, the compactness is a key factor, which is usually expressed by the Colburn factor, j , given as [1]:

$$j = \frac{D_h}{4L} \text{Pr}^{2/3} N \quad (1)$$

To develop advanced compact heat exchangers, it is necessary to improve the thermal performance, so that reduce the hydraulic diameter as well as the core volume. The printed circuit heat exchanger (PCHE) is a new type heat exchanger with high compactness and efficiency. It is composed of multilayer metal plates with chemical etching channels, where fluid-flows and heat transfer proceeds. Supercritical CO₂ (S-CO₂) has received a great deal of interest attributing to its excellent thermal performance and high cycle efficiency. Therefore, it has been widely used in gas turbine cycle [2] and energy systems.

* Corresponding author, e-mail: yhxie@mail.xjtu.edu.cn

During recent years, researchers have presented many studies on the thermal hydraulic performance of PCHE. Kim *et al.* [3] conducted experimental and numerical investigations on the thermal hydraulic performance of PCHE based on helium cycle. Then Kim *et al.* [4] numerically investigated the heat exchange performance of PCHE with longitudinal corrugation flow channels. Figley *et al.* [5] simulated the heat transfer characteristics of PCHE in the laminar-to-turbulent transition flow condition. It was illustrated that the corresponding transition Reynolds number for semi-circular and circular channels were 3100 and 2300, respectively. Mylavarapu *et al.* [6] investigated the hydraulic performance of PCHE using the high temperature helium test facility in Ohio State University Columbus, O., USA. For the convenience of research, reduced-scale PCHE with Z shape channels were constructed using alloy 617 by Chen *et al.* [7]. Furthermore, the phase transition condensation characteristics in Z shape channel were simulated by Lai *et al.* [8].

With the development of S-CO₂, some researchers introduced the S-CO₂ into PCHE and carried out a series of investigations. Nikitin *et al.* [9] studied the heat transfer and friction characteristics of PCHE in S-CO₂ experimental loop. Ngo *et al.* [10] developed a new type PCHE with many discontinuous S-fins. Tsuzuki *et al.* [11] compared the thermal hydraulic performance of new type PCHE with that of conventional Z shape channel, and found that the pressure drop was reduced to 20%. Moreover, the PCHE with airfoil fins was proposed by Kim *et al.* [12]. Xu *et al.* [13] carried out optimization research on heat transfer characteristics of airfoil fins PCHE. Jeon *et al.* [14] creatively presented the heterogeneous PCHE, for which the effects of channel size and the cross-section shape were numerically investigated.

From the open literatures, it can be found that researchers have shown great interest in the S-CO₂ PCHE because of the excellent thermal hydraulic performance and extensive application background. Those researchers focused on the Z shape, S-fins and airfoil fins PCHE. While for S shape channels with different bend angle and the comparisons with Z shape and straight channels, only a few papers have been presented. Therefore, more comprehensive and detailed data are necessary. In this paper, the numerical investigations have been carried out on the flow patterns and thermal hydraulic performances of Z and S shape PCHE with different channel bend angle. Based on the S-CO₂ Brayton cycle described in reference [11], the Z and S shape channels are modeled. By analyzing the effects of channel shape and bend angle, the corresponding laws have been obtained.

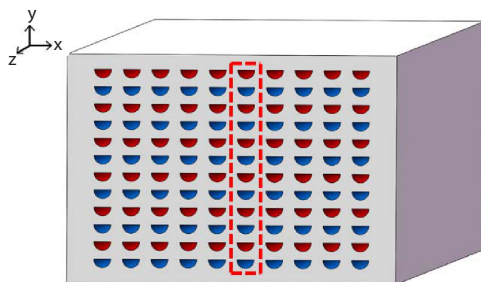


Figure 1. Schematic diagram of PCHE

Figure 2(a) shows the dimensions of straight channel. The width, W , and height, H , of solid domain are 4 mm and 4.8 mm, respectively. For hot and cold channels, the radius of cross-section R_h and R_c are both 1.2 mm. The channel length, L , is 240 mm. Figure 2(b) dis-

Physical model and numerical method

Physical model

The schematic diagram of PCHE is shown in fig. 1, which is composed of multilayer metal plates with chemical etching channels (where hot channels are colored with red, cold channels are colored with blue). The present investigation focuses on one column of the heat exchanger, shown in red dash box. Besides, the period domain is built as the calculated model, which consists of solid regions, one hot channel and one cold channel with semi-circular cross-sections.

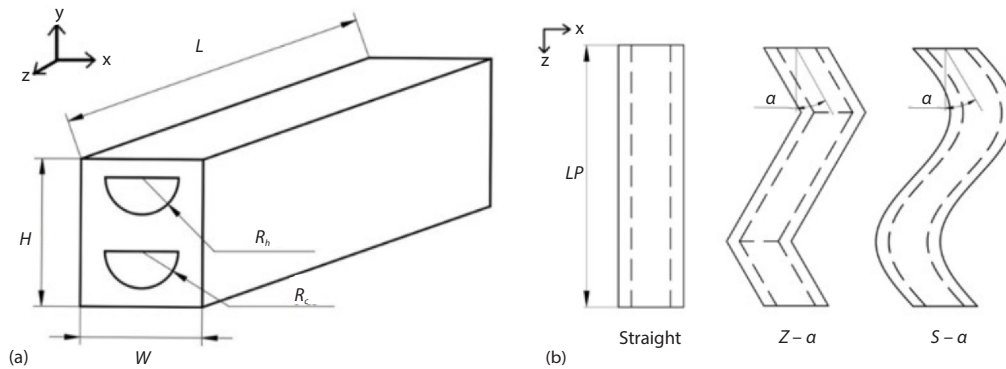


Figure 2. (a) Dimensions of straight channel, (b) three different shapes of fluid channel

plays the geometries of three different shapes for fluid channel in the flow direction, including straight, zig-zag, Z, and sinusoidal, S. For those channels, the geometries are determined by length pitch LP (16 mm) and bend angle α (10° , 20° , and 30°). In this paper, a total of seven different shaped channels are studied, including straight, Z-10, Z-20, Z-30, S-10, S-20, S-30.

Numerical method

For PCHE in this paper, the material of heat exchanger plate is 617 alloy [15] and CO_2 flows in the semi-circular channels for both sides. The top and bottom surfaces are periodic boundaries and two side surfaces are set as adiabatic walls. The inlet temperature and outlet pressure are 553K/2.6 MPa for hot channel and 381K/8.5 MPa for cold channel, respectively. The mass-flow rates according to specific Reynolds number varying from 5000-30000 are utilized at the inlets of hot and cold channels. Additionally, the front and back surfaces of solid region are both adiabatic walls.

The commercial software FLUENT 15.0 is adopted for numerical calculation. The integrated NIST real gas model is used to simulate the dramatic change of physical properties for S- CO_2 . For solid region, the constant physical properties are adopted. All equations are solved using second-order upwind discretization, and pressure and velocity are coupled using the semi implicit method pressure linked equation (SIMPLE).

In this paper, the mesh is generated using hexahedral division strategy by ANSYS ICEM CFD. The O shaped topology is adopted for the semi-circular cross-section, and the grids are densified near the fluid-solid coupled surfaces. Comprehensively considering the accuracy and efficiency of simulations, the grid dependence study is performed with Z-30 channel, shown in tab. 1. Four grid schemes are considered, for which the outlet temperature and pressure drop of hot channel are compared. Finally, mesh 3 is adopted and the node number is 4.77 million.

Table 1. Grid dependence study with Z-30 channel, hot side

Mesh scheme	Node (10^4)	$T_{h,out}$ [K]	Error [%]	Δp_h [Pa]	Error [%]
1	93	424.4	0.69	4870.8	0.63
2	258	421.5	0.38	4901.8	0.58
3	477	419.9	0.29	4930.3	0.23
4	760	418.7		4941.5	

The FLUENT 15.0 has provided many turbulence models. From the experimental and numerical investigations of reference [11], it can be found that the RNG $k-\varepsilon$ model can accurately simulate the flow and heat transfer of S-CO₂ in PCHE. Therefore, RNG $k-\varepsilon$ model is adopted in the present study.

The Reynolds number is defined:

$$\text{Re} = \frac{\rho u_{in} D_h}{\mu} \quad (2)$$

The hydraulic diameter of fluid channel is:

$$D_h = \frac{\pi D_{ch}}{\pi + 2} \quad (3)$$

The Nusselt number is defined:

$$\text{Nu} = \frac{h D_h}{\lambda} = \frac{q}{T_w - T_f} \frac{D_h}{\lambda} \quad (4)$$

The friction factor is defined:

$$f = \frac{\Delta p D_h}{2 \rho L u_{in}^2} \quad (5)$$

The heat exchanger effectiveness η is:

$$\eta = \frac{T_{h,in} - T_{h,out}}{T_{h,in} - T_{c,in}} \quad (6)$$

Results and discussion

The temperature variations along the channel length for Z-30 channel at the Reynolds number of 10000 are shown in fig. 3(a). It can be observed that, in the flow direction, the temperature variations of hot CO₂ and cold S-CO₂ are both approximately linear along the channel. Owing to the continuous heat transfer, the temperature decreases in the hot side while increases in the cold side. The pressure drop variations along the channel length are plotted in fig. 3(b).

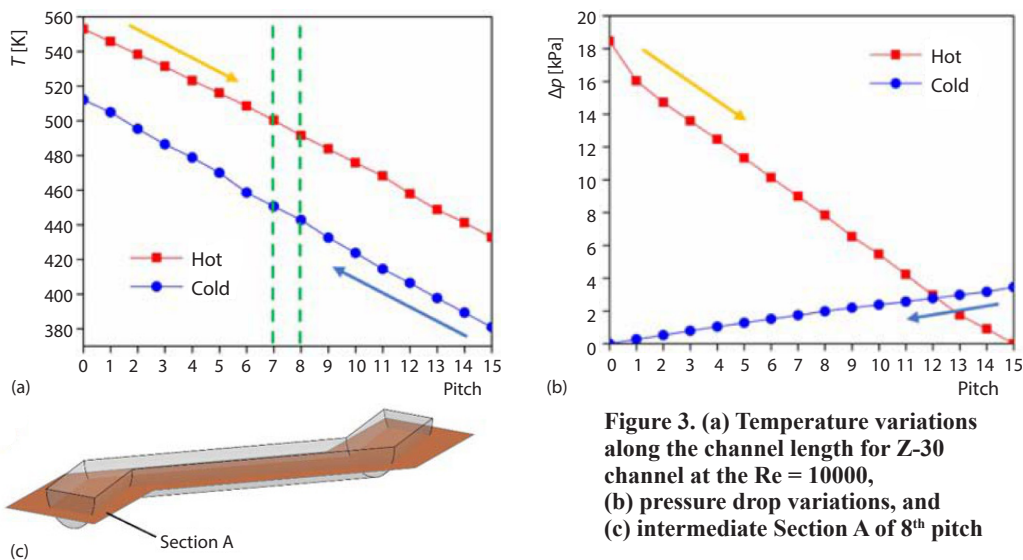


Figure 3. (a) Temperature variations along the channel length for Z-30 channel at the $\text{Re} = 10000$, (b) pressure drop variations, and (c) intermediate Section A of 8th pitch

Similarly, the pressure drop variations are approximately linear. The pressure of hot side drops faster than that of cold side, indicating that the properties of hot fluid fluctuate more violently.

The 8th pitch, between dashed line in fig. 3(a), of the channel has been shown in fig. 3(c) with intermediate Section A. The streamlines and temperature distributions of Section A for Z shape channels are shown in fig. 4. The left sides are hot channels and the right sides are cold channels. The bend angle varies from 10-30° and the $Re = 10000$. It can be found that the streamlines of Z-10 cold side are uniform resulting from the small bend angle, which attributes to the global low temperature. For Z-20 cold channel, at the bend region, the stream lines are grouped in the inner areas while leaving sparse streamlines in the outer areas due to the increase of bend angle. It can be also seen that high temperature regions are produced after the turning bend, suggesting that the adopt of turning bend effectively enhances the flow mixing and breaks the flow boundary-layer, thus improving the heat transfer. As for Z-30 cold channel, the streamlines become more uneven and fluid separates right after the turning bend with vortices grouped in the inner side.

Figure 5 shows the streamlines and temperature distributions of Section A for S shape channels, for which the left figures are hot channels and the right figures are cold channels. The bend angle varies from 10-30° and the $Re = 10000$. It can be seen that the streamlines of S shape channels are more uniform than that of Z shape channels, attributing to the smooth transition. With the increase of bend angle, the inner streamlines near the turning bend become denser while the outer streamlines become sparse. Besides, the global temperature of cold side increases slowly, which is similar to that of Z shape channel.

As the bend angle reaches 30°, there is still not flow separation for S shape channel, suggesting that the S shape channel produces less flow resistance with the equivalent heat transfer enhancement, compared with Z shape channel. This is because that the S shape channels do not have sharp turning bend, where the fluid flushes the wall and flows downstream along the smooth arcs. On

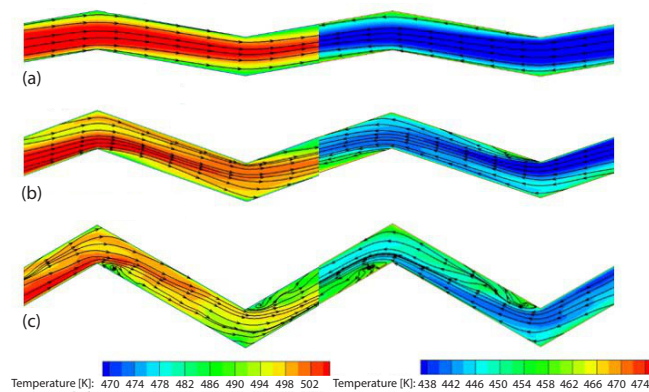


Figure 4. Streamlines and temperature distributions of Section A for Z shape channels, $Re = 10000$; (a) Z-10 channel, (b) Z-20 channel, and (c) Z-30 channel

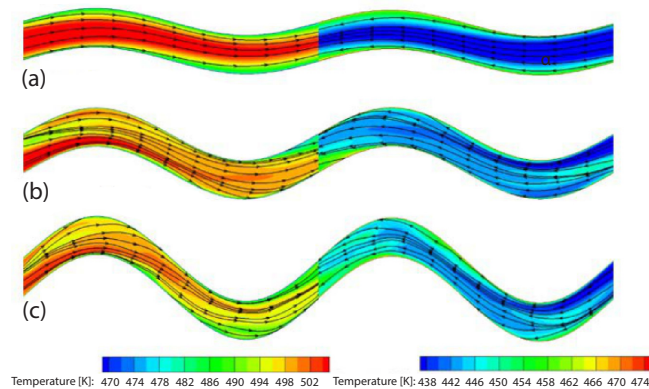


Figure 5. Streamlines and temperature distributions of Section A for S shape channels, $Re = 10000$; (a) S-10 channel, (b) S-20 channel, and (c) S-30 channel

the comprehensive consideration of flow patterns and temperature distributions, S shape channel exhibits more obvious advantages.

Figure 6(a) shows the Nusselt number variations with Reynolds number for different channels in the cold side. It can be seen that the Nusselt number of all cases has little difference at low Reynolds number, while the difference increases with Reynolds number. Clearly, the straight channel produces the smallest Nusselt number. The Nusselt number increases with larger bend angle (10° and 20°). The Nusselt number of S shape channel is slightly higher than that of Z shape channel. At the bend angle of 30° , the maximum deviation of Nusselt number between Z and S shape channels is only 5.58% within the $Re = 10000$, as Reynolds number increases, the Nusselt number of Z shape channel is significantly higher than that of S-shape channel. Overall, the Nusselt number of S-30 channel is improved by 16.93-40.39% relative to straight channel while the Nusselt number of Z-30 channel is improved by 19.12-55.60%. Figure 6(b) shows the friction factor variations with Reynolds number for different channels in the cold side. Obviously, the f decreases with Reynolds number for all cases. The f of Z-30 channel is 3.25-7.57 times that of straight channel, while the S-30 channel only produces 3.57 times the f of the straight channel at most. Moreover, it can be also determined that f increases with larger bend angle, simultaneously, the Z shape channels produce larger f compared with S shape channels under the same bend angle. Synthetically considering the heat transfer and friction characteristics, it is concluded that, compared with channel shape, the bend angle plays a more important role in the thermal hydraulic performance. By comparisons of Nusselt number and f for all cases, the S-20 channel presents the best thermal hydraulic performance.

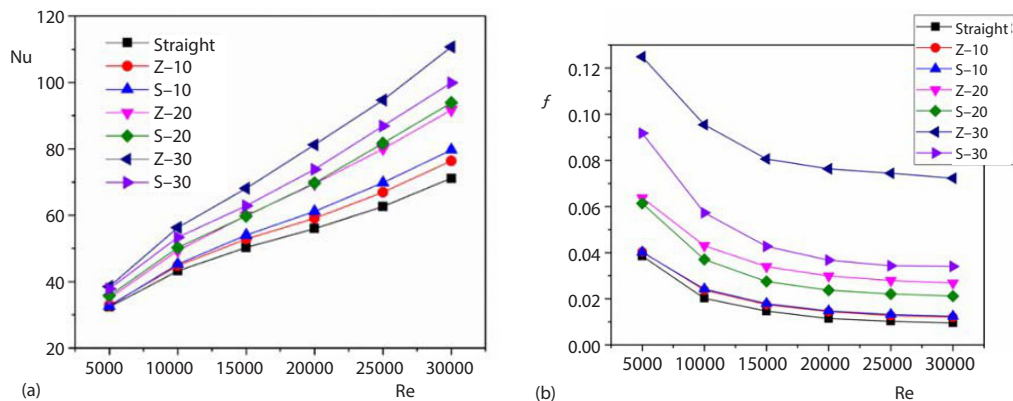


Figure 6. The Nu and f variations with Re for different channels in the cold side

The variations of heat exchanger effectiveness η with Reynolds number for different channels are shown in fig. 7. It is obvious that, for all cases, the η decreases with larger Reynolds number. Meanwhile, the downward trend is gradually easing, resulting from the combined effects of heat transfer intensity and heat exchange time. In addition, the bend angle plays a major role in the heat exchanger effectiveness. The S shape channels produce larger η than Z shape channels under the bend angle of 10 - 20° . At the bend angle of 30° , the η of S shape channel is slightly higher than that of Z shape channel at the $Re = 5000$ and with the increase of Reynolds number, the Z shape channel presents better heat exchanger performance. This is because that larger flow rate enhances the impingement effect in the bend region for Z shape channel, which is relatively weak in S shape channel. Comprehensively, the S-30 channel produces the best heat exchange performance with the maximum η of 77.4%.

Conclusion

In this paper, the thermal fluid-solid coupling models of PCHE are constructed and numerical calculations are conducted to investigate the effects of channel shape, bend angle and Reynolds numbers on the thermal hydraulic performance. The flow patterns, heat transfer and friction characteristics of Z and S shape channels are obtained.

- The investigation suggests that small bend angle produces uniform streamlines. As bend angle increases, the streamlines are grouped in the inner areas while leaving sparse streamlines in the outer areas. For Z-30 channel, the vortices are produced right after the turning bend. While in S shape channels, no flow separation is produced within the bend angle range of 10-30°.
- The Nusselt number increases and friction factor, f , decreases with larger Reynolds number for all cases. The thermal hydraulic performance is more sensitive to the bend angle. Larger bend angle results in higher Nusselt number and f . Under the same bend angle, the S shape channels produce slightly higher Nusselt number and lower f than Z shape channels. Specifically, the Nusselt number of S-30 channel is improved by 40.39% at most with 3.57 times f , based on straight channel.
- The heat exchanger effectiveness, η , decreases with larger Reynolds number. The S shape channels produce larger η than Z shape channel at the same bend angle and Reynolds number. Comprehensively, the S-30 channel produces the best heat exchange performance with the maximum η of 77.4%. While considering the Nusselt number and f , S-20 produces the best comprehensive thermal hydraulic performance.

Acknowledgment

This work was supported by the Foundation of the Key Laboratory of Thermal Power Technology (TPL2016BA001).

Nomenclature

D_{ch} – diameter of fluid channel, [mm]
 D_h – hydraulic diameter, [mm]
 f – channel friction factor, [-]
 H – height of solid domain, [mm]
 h – heat transfer coefficient, [$Wm^{-2}K^{-1}$]
 j – Colburn factor, [-]
 L – channel length, [mm]
 LP – length pitch, [mm]
 N – thermal unites number, [-]
 Nu – Nusselt number, [-]
 Pr – Prandtl number, [-]
 Δp – pressure drop, [Pa]
 q – wall heat flux, [Wm^{-2}]

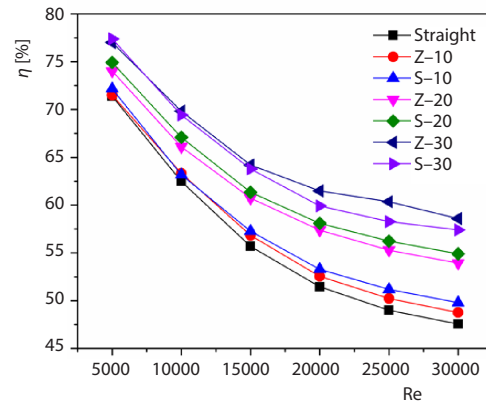


Figure 7. Variations of heat exchanger effectiveness η with Re for different channels

Re – Reynolds number, [-]
 R_c – radius of cold channel, [mm]
 R_h – radius of hot channel, [mm]
 T – temperature, [K]
 u – flow velocity, [ms^{-1}]
 W – width of solid domain, [mm]

Greek symbols

α – channel bend angle, [°]
 η – heat exchanger effectiveness, [-]
 λ – fluid thermal conductivity, [$Wm^{-1}K^{-1}$]
 μ – fluid dynamic viscosity, [Pa·s]
 ρ – fluid density, [kgm^{-3}]

References

- [1] Hesselgreaves, J. E., *Compact Heat Exchangers: Selection, Design and Operation*, Pergamon Press, Oxford, UK, 2001
- [2] Kato, Y., *et al.*, Medium Temperature Carbon Dioxide Gas Turbine Reactor, *Nuclear Engineering and Design*, 230 (2004), 1-3, pp. 195-207
- [3] Kim, I. H., *et al.*, Thermal Hydraulic Performance Analysis of the Printed Circuit Heat Exchanger Using a Helium Test Facility and CFD Simulations, *Nuclear Engineering and Design*, 239 (2009), 11, pp. 2399-2408
- [4] Kim, J. H., *et al.*, Hydraulic Performance of a Micro-channel PCHE, *Applied Thermal Engineering*, 30 (2010), 14, pp. 2157-2162
- [5] Figley, J., *et al.*, Numerical Study on Thermal Hydraulic Performance of a Printed Circuit Heat Exchanger, *Progress in Nuclear Energy*, 68 (2013), Sept., pp. 89-96
- [6] Mylavarapu, S. K., *et al.*, Thermal Hydraulic Performance Testing of Printed Circuit Heat Exchangers in a High-Temperature Helium Test Facility, *Applied Thermal Engineering*, 65 (2014), 1-2, pp. 605-614
- [7] Chen, M. H., *et al.*, Pressure Drop and Heat Transfer Characteristics of a High-Temperature Printed Circuit Heat Exchanger, *Applied Thermal Engineering*, 108 (2016), Sept., pp. 1409-1417
- [8] Lai, Z. C., *et al.*, Numerical Simulation of Refrigerant Flow Condensation Characteristics in Zig-zag Channel of Printed Circuit Heat Exchanger, *Chinese Journal of Refrigeration Technology*, 36 (2016), 4, pp. 29-35
- [9] Nikitin, K., *et al.*, Printed Circuit Heat Exchanger Thermal-Hydraulic Performance in Supercritical CO₂ Experimental Loop, *International Journal of Refrigeration*, 29 (2006), 5, pp. 807-814
- [10] Ngo, T. L., *et al.*, New Printed Circuit Heat Exchanger with S-Shaped Fins for Hot Water Supplier, *Experimental Thermal and Fluid Science*, 30 (2006), 8, pp. 811-819
- [11] Tsuzuki, N., *et al.*, High Performance Printed Circuit Heat Exchanger, *Applied Thermal Engineering*, 27 (2007), 10, pp. 1702-1707
- [12] Kim, D. E., *et al.*, Numerical Investigation on Thermal-Hydraulic Performance of New Printed Circuit Heat Exchanger Model, *Nuclear Engineering and Design*, 238 (2008), 12, pp. 3269-3276
- [13] Xu, X. Y., *et al.*, Optimization of Fin Arrangement and Channel Configuration in an Airfoil Fin PCHE for Supercritical CO₂ Cycle, *Applied Thermal Engineering*, 70 (2014), 1, pp. 867-875
- [14] Jeon, S., *et al.*, Thermal Performance of Heterogeneous PCHE for Supercritical CO₂ Energy Cycle, *International Journal of Heat and Mass Transfer*, 102 (2016), Nov., pp. 867-876
- [15] Li, X. Q., *et al.*, Alloy 617 for the High Temperature Diffusion-Bonded Compact Heat Exchangers, *Proceedings, ICAPP '08*, Anaheim, Cal., USA, 2008